

RSC Advances



This is an *Accepted Manuscript*, which has been through the Royal Society of Chemistry peer review process and has been accepted for publication.

Accepted Manuscripts are published online shortly after acceptance, before technical editing, formatting and proof reading. Using this free service, authors can make their results available to the community, in citable form, before we publish the edited article. This *Accepted Manuscript* will be replaced by the edited, formatted and paginated article as soon as this is available.

You can find more information about *Accepted Manuscripts* in the [Information for Authors](#).

Please note that technical editing may introduce minor changes to the text and/or graphics, which may alter content. The journal's standard [Terms & Conditions](#) and the [Ethical guidelines](#) still apply. In no event shall the Royal Society of Chemistry be held responsible for any errors or omissions in this *Accepted Manuscript* or any consequences arising from the use of any information it contains.

Engineering a functional neuro-muscular junction model in a chip

Cite this: DOI: 10.1039/x0xx00000x

Ziqiu Tong,^{‡^a} Oscar Seira,^{‡^{ab}} Cristina Casas,^a Diego Reginensi,^{abc} Antoni Homs-Corbera,^{ade} Josep Samitier^{ade} and José Antonio Del Río^{abc}

Received 00th January 2012,
Accepted 00th January 2012

DOI: 10.1039/x0xx00000x

www.rsc.org/

Healthy bi-directional intracellular transport along the axons between the somatodendritic and synaptic terminals is crucial to maintain the function and viability of neurons. When misbalanced, there is neuronal homeostasis failure that compromises its function and viability. In fact, several neurodegenerative diseases are originated from misbalanced axonal transport and function. Thus numerous techniques have been developed to establish and maintain neuronal cultures in compartmented microfluidic devices to better understand these processes mimicking neuronal polarization. Although useful, these *in vitro* platforms do not allow for a full specific and temporal analysis in a complete monitored way. In this study, we have utilized a microfluidic system with large open cell culture reservoirs to precisely control neuronal microenvironments, capable of mimicking axon transport and synapse formation and to facilitate their analysis. We demonstrate using this lab-on-a-chip system for long-term motoneuron co-culture with C2C12-derived myotubes to mimic neuro-muscular junction (NMJ) formation. Furthermore, by integration with calcium (Ca²⁺) imaging technique, we have proved the NMJ functionality in-chip through KCl-induced Ca²⁺ transient in connected myotubes. This platform can potentially become a useful tool as a straight forward, reproducible, and high-throughput *in vitro* model for basic NMJ research, and for high-throughput drug screening.

Introduction

Neuronal polarization is a key process during neuronal differentiation and maturation being the basis of neuronal transmission.¹ The signal propagation depends on the fact that neurons display two morphologically and functionally distinct domains: the somatodendritic and axonal domains.² During maturation, especially in the adult stage, neurons maintain their polarity by controlling local protein synthesis and degradation together with axonal transport along their microtubule-enriched

cytoskeleton.³⁻⁵ In fact, most neuronal functions rely on the relevant bi-directional long-distance transport of cytoplasmic components including vesicles, mitochondria and endocytic organelles along the axon.¹ The maintenance of these domains, in particular the axonal functions, are especially crucial in long-range projecting neurons such as spinal motor neurons or cortical pyramidal cells. Indeed, given the importance of polarity, many studies have focused on uncovering the mechanisms that establish neuronal polarization, and many factors involved in axon specification have been identified using *in vitro* and *in vivo* models. For example, organelle (mitochondria) transport along axons has attracted special interest in recent years following its influences on neurodegenerative diseases in both central⁶⁻⁸ (i.e., Alzheimer's or Parkinson's diseases) and peripheral^{9,10} nervous system (i.e., Amyotrophic Lateral Sclerosis or Charcot-Marie-Tooth diseases).

Precise control, manipulation, and monitoring of cellular microenvironments using microfluidics technology, enabling the handling of fluid flow at μ -meter scale, has becoming an indispensable tool for biomedical researchers. Especially those presenting compartmentalized microfluidic platforms which enable the physical isolation of axons from cell bodies and dendrites, have gained much popularity in neurobiological research¹¹ (ESI Table 1†). Their applications have revealed novel findings that have otherwise been unobtainable by other

^aInstitute for Bioengineering of Catalonia (IBEC), Baldiri Reixac 15-21, 08028 Barcelona, Spain. Tele: +34 93 4035923; Emails: jadelrio@ibecbarcelona.eu, jsamitier@ibecbarcelona.eu

^bCentro de Investigación Biomédica en Red de Enfermedades Neurodegenerativas (CIBERNED), Barcelona, Spain.

^cDepartment of Cell Biology, University of Barcelona (UB), Barcelona, Spain

^dCentro de Investigación Biomédica en Red de Bioingeniería, Biomateriales y Nanomedicina (CIBER-BBN), Zaragoza, Spain

^eDepartment of Electronics, Universitat de Barcelona, Barcelona, Spain
‡Current address: International Collaboration On Repair Discoveries (ICORD) Blusson Spinal Cord Centre and Department of Zoology, Faculty of Science, University of British Columbia, Vancouver, Canada.

‡Authors equally contributed to the work

†Electronic Supplementary Information (ESI) available: See DOI: 10.1039/b000000x/

in vitro or *in vivo* methods. For example, a dual compartmentalized microfluidic cell culture device was used by Taylor *et al.* to extract selectively the axonal mRNA from mammalian CNS neuron.¹² Current studies have also focused on using this or similar compartmentalized microfluidic devices to investigate axon growth,^{13,14} axon-glia interaction,¹⁵ axon responses in models of spinal cord injury¹⁶ or synapse junction screening¹⁷ (ESI Table 1†). In addition, when combined with microelectrode array platform, these devices have been utilized to examine the cortico-thalamic network¹⁸ and to assess cortico-cortical electrical activity.¹⁹ Traditional method to establish NMJ formation requires motoneurons and muscle cells to be seeded in the same petri dish and co-cultured under single culture medium.^{20,21} Recent attempts have been made to utilize aforementioned compartmentalized microfluidic systems to create more suitable *in vitro* models.^{22,23} In fact, in the organism cell bodies of motoneurons are located meters away from the muscle cells and both experience different physiological microenvironments. Hence, it is inadequate to faithfully recapitulate *in vivo* condition of the neuromuscular connections via traditional petri dish co-culture approach. Furthermore, to manipulate individual cell population within the mixed population seems difficult.

The ability to tailor cell microenvironments individually can be desirable and useful, and usually mimics more closely the physiological conditions. Based on the microfluidic co-culture system developed by Taylor *et al.*,²⁴ in a scale similar to the pioneering study by Campenot,²⁵ we have utilized a microfluidic chip compatible with the size and geometry of a microscope slide for further optical analysis. The compartmented system contains a physical barrier with a large number (up to 200) of embedded microchannels separating two identical compartments that permits only the extension of neurites. In addition, controlled, fluidically isolated cell seeding reservoirs have been achieved in our device by simple control of media volume differences between the two reservoirs. Furthermore, this type of open system provides an easier and more direct access to manipulate cell cultures.^{26,27}

We report in here a robust co-culture protocol of mouse primary motoneuron cells with C2C12-derived myotubes in our modified chip. We have successfully demonstrated the synaptic formation between the two cell types by bungarotoxin (BTX) immunostaining,^{22,23} and we have further integrated the calcium imaging technique to study the functional synapse responses, namely to chemically stimulate motoneurons and observe calcium influx changes in differentiated myotubes.

Materials and methods

Neuron culture device design and fabrication

Microfluidic neuron culture platform was fabricated in poly(dimethylsiloxane) (PDMS) by standard photolithography and soft lithography.³⁸ The overall chip design and dimensions can be seen in Figure 1. Polystyrene transparent masks were designed using CAD file and printed via a high-resolution printer (CAD/Art Services, OR, USA). For the fabrication of single 2 μm wide channel chip, a chrome mask (JD Photo-Tools, United Kingdom) was instead used for achieving a higher resolution.

In brief, a glass slide was pre-cleaned by immersing in Piranha solution for 10 minutes and dried at 200° C for 30 minutes. SU8 2 (Microchem, MA) photoresist was then spun at a rate of 5000 rpm for 30 seconds to obtain a thin-film layer (1 μm thick) which facilitates the adhesion of subsequent layers of

photoresist. The resulting photoresist coated glass slide was exposed with UV light for 10 seconds and heated for 1 minute at 95°C. A second layer of SU8 2 was then spin-coated at a rate of 1500 rpm to achieve a thickness of approximate of 2.7 μm . A polystyrene transparent mask defining the microchannels (10 μm width by 50 μm spacing, Fig. 1) was then used to pattern the second layer of SU8 2 by exposing to UV light for 4.5 seconds. In the case of fabricating 2 μm wide channels, a chrome mask was used and exposed to UV light for 3 seconds. After resolved with SU-8 Developer (MicroChem), the master was rinsed with isopropanol (Panreac Quimica, Spain), and dried with nitrogen gas. The process was repeated with a denser photoresist to create the third layer of two reservoirs. SU8 50 was spun at 2000 rpm for 30 seconds (resulting 60 μm in height) and a second polystyrene transparent mask was aligned to the first pattern and used to pattern the two large reservoirs. The final SU8 on glass structure was used to create a replication process resistant mold of PDMS by a pouring and casting methodology.

The slide was treated with Trichloro(1H,1H,2H,2H-perfluorooctyl)silane (Sigma) for 1 hour before pouring PDMS mixture onto it. A thin layer slab of PDMS (1 mm) was fabricated by mixing a small amount of 10:1 ratio of PDMS base to catalyst, and poured onto the silanized SU8 master. Then, it was subjected to curing by oven heating for 1 hour at 85°C. The cured PDMS was carefully peeled from the SU8 structure thus creating a PDMS-master. The master was then placed inside the plasma cleaner (Harrick Scientific, NY) for 1 min to activate the surface, and then irreversibly bound to a glass slide (also treated with plasma) with the non-feature side contacting the glass to be used later to make replicas of final PDMS device (5 mm thick). The advantage of using a PDMS master is that it's more robust and durable than the SU8 photoresist features on glass. Two large cell-seeding reservoirs were hollowed out by using Harris Uni-Core cutter ($\varnothing = 12$ mm, Ted Pella, CA). The final PDMS devices were cleaned by sonication in ethanol and then in Milipore water, and were further sterilized by autoclaving process.

Features of SU8 on glass and PDMS chips were analyzed and verified by mechanical profilometer (DEKTAK 6M, Veeco, NY), optical profilometry (WYKO NT1100, Veeco, NY), or scanning electron microscopy (SEM) (FEI, Oregon) before their subsequent uses.

Device surface coating

Thin glass cover slides (24x60mm, Menzel Gläser, Germany) were cleaned with ethanol and sterilized in an autoclave. The PDMS culture chips and glass cover slides were surface-activated by introducing inside a plasma cleaner for 2 minutes. Then the PDMS chips were assembled on top of the cover slides by applying gentle pressure with a pair of tweezers. The bonded devices were further sterilized under UV light for 10 minutes inside a cell culture hood before pipetting coating solution of Poly-L-Ornithine (15 $\mu\text{g}/\text{mL}$, Sigma) and then incubated for 3 hours at room temperature (RT) until dry. Next, laminin (3 $\mu\text{g}/\text{mL}$, Sigma) was added to the wells and stored overnight in a humidified incubator (37°C, 5% CO₂). The devices were washed three times with Mili-Q water and PBS before seeding cells.

Mouse embryonic motoneurons isolation

Motoneuron-enriched cultures were isolated from ventral cords of embryonic day 13.5 (E13.5) mice. Animals were maintained in a pathogen-free barrier facility at the University of Barcelona

animal facility. Experiments were approved by the University of Barcelona Animal Care (Protocol 7855) and Use Committee and used in accordance with Spanish (RD223/88) and European (86/609/ECC) regulations. Ventral spinal cord tissue was dissected from embryos and collected in cold dissection media (Hank's balanced salt solution, HBSS, Invitrogen Life Technologies) containing 6.5 mg/ml culture grade glucose (Sigma). The tissues were mechanically chopped and dissociated with 0.05 % trypsin-EDTA (Invitrogen Life Technologies) for 7 minutes at 37°C. Fragments were collected and transferred to an L15 solution (Invitrogen Life Technologies) with B27 (18 mM Glucose/22.5 mM NaHCO₃/antibiotics and N2 supplement) mixed with 4% BSA (Sigma) and 1mg/mL DNase I (Applied Biosystems) solutions. Tissue fragments were then mechanically dissociated with a pipette tip (200 µl) and the dispersed cell suspension was left standing for 2 minutes to precipitate the tissue debris. The supernatant was collected in a new conical tube and the dissociated cells were layered over a 1.5 mL of L15 solution with 4% BSA followed by centrifugation at 200 xg for 5 minutes at RT for the first purification step. The pellet was then re-suspended and layered over a 2 mL gradient solution with dissection media and OptiPrep density gradient medium (60%, Axis-Shield) followed by centrifugation at 520 xg for 10 minutes at RT. The final pelleted motoneurons were suspended in a complete motoneuron media (CMM) and were ready for seeding in glass bottom petri dishes (Ø = 12 mm) or in the somal compartments of the microfluidic devices.

C2C12 myoblast culture and preparation

C2C12 cells were expanded in DMEM supplemented with 10% FBS (Invitrogen Life Technologies), 25 mM HEPES (Invitrogen Life Technologies), 1% L-glutamine, and antibiotics. When culture reached 90% confluence, FBS serum was replaced to 5% normal horse serum (NHS) in order to trigger myotube differentiation.

Co-culture of motoneurons and C2C12 muscle cells in microfluidic chip

Motoneurons were seeded first in the compartmentalized devices (~4.5-5x10⁵ cells/compartiment) and maintained in CMM containing Neurobasal media, supplemented with 1% NHS, 1% penicillin/streptomycin, B27 and L-glutamine (all from Invitrogen Life Technologies). Ciliary Neurotrophic Factor (CNTF, 10 ng/mL, PeproTech) and Glial-Derived Neurotrophic Factor (GDNF, 10 ng/mL, PeproTech) were added to CMM. On the next day, C2C12 myoblasts were seeded in the myotube compartments (~2000 cells/compartiment) and cultured in C2C12 media. 3 days later, media was replaced with differentiation media to induce myoblast differentiation. Meanwhile, cytosine arabinoside (Ara-C, 5 µM, Sigma) was added to the CMM to suppress excessive glial cell growth. Co-cultures were maintained until C2C12 cells were highly differentiated to myotubes and motoneuron axons reached the myotube compartments which were usually detected at 8-10 DIV. Media changes for both cultures were carried out every 3 days. For C2C12 myotube culture, 3-4 days after differentiation started, the media was also supplemented with Ara-C to prevent myoblasts from dividing and becoming overcrowded. From that point on, the co-cultures were ready for subsequent analysis with CalceinTM (1 mM, Molecular Probes), Mitotracker labeling (200 nM, Invitrogen Life Technologies) or use for confocal Ca²⁺ influx measurements. In selected experiments, additional neurotrophins: Brain Derived Neurotrophic Factor (BDNF, 2

ng/ml, PeproTech) and Hepatocyte Growth Factor (HGF, 10 ng/ml, PeproTech), or inhibitory molecules: Semaphorin 3A (Sema3A, 1 µg/ml, R&D systems) were added to the motoneuron culture media to access the axon growth efficiency.

Immunostaining and Alexa-Bungarotoxin staining

Cell cultures were fixed in 4% buffered paraformaldehyde for 30 minutes at RT, washed twice in 0.1 M PBS, and then permeabilized with 0.2% Triton X-100 in 0.1 M PBS for 10 minutes. Cultures were blocked with 10% FBS in 0.1 M PBS for 30 minutes at RT. Primary antibody dilutions were prepared as followed: monoclonal anti-myosin (Sigma) was diluted at 1:1000 and polyclonal anti-β-tubulin (Covance) at 1:2000. The Alexa Fluor 488-conjugated α-bungarotoxin (Alexa-BTX; 1:1000, Molecular Probes) was used to visualize the acetylcholine receptor (AChR) clusters present in the NMJs. Cultures were incubated in primary antibodies diluted in 0.1 M PBS containing 5% FBS at 4°C overnight or for 1 hour at RT. Cultures were then rinsed 3 times with 0.1 M PBS and incubated for 90 minutes at RT with secondary antibodies (Alexa Fluor 488, 568, 405, 1:500; Molecular Probes) diluted in 0.1 M PBS. To increase the efficiency of labelling and washing, the amount of solutions in the microfluidic chip compartments were kept at some differences. The hydrostatic pressure caused by the fluid height difference facilitated the fluids entering the microchannels. Images were acquired by Leica TCS SP5 confocal microscopy or Olympus BX61 microscopy and were further analyzed and processed by ImageJ^R software.

Calcium (Ca²⁺) transient measurement

Myotube compartments containing differentiated myotubes were rinsed twice with HBSS and then incubated with a calcium sensitive fluorescent dye, Fluo-4 acetoxymethyl (Fluo-4 AM) ester (10 µM, Invitrogen Life Technologies) for 1 hour at 37°C. After the incubation, Fluo-4 AM was removed and rinsed three times with HBSS. The co-culture chips were then incubated for another 30 minutes at 37°C in HBSS for de-esterification process before performing fluorescence measurements. Potassium chloride (KCl, 100 mM, Sigma) was added to motoneuron compartments as a depolarization agent. Ca²⁺ release intensity level in myotube compartments was recorded for a total of 30 minutes. The liquid volumes in myotube compartments were kept higher than the motoneuron compartments to prevent the convective flow of KCl to myotube compartments. As a positive control, after 30 minutes video recording, KCl was added directly to the myotube compartments. In selected experiments, Tetrodotoxin (TTX, 2 µM, Sigma) was added to the motoneuron compartment after the initial KCl stimulation. During whole labelling process, motoneuron compartments were always maintained with the motoneuron growth media. The fluorescence intensity time-lapse videos were acquired using Leica TCS SP2 confocal microscopy equipped with temperature (37°C), humidity, and CO₂ controls. The images were further analyzed and quantified with ImageJ^R software (MBF plugin, McMaster University biophotonics facility).

Results

Design and fabrication of the neuronal microfluidic co-culture platform

The microfluidic co-culture platform consists of a moulded elastomeric polymer piece, PDMS, placed on top of a glass

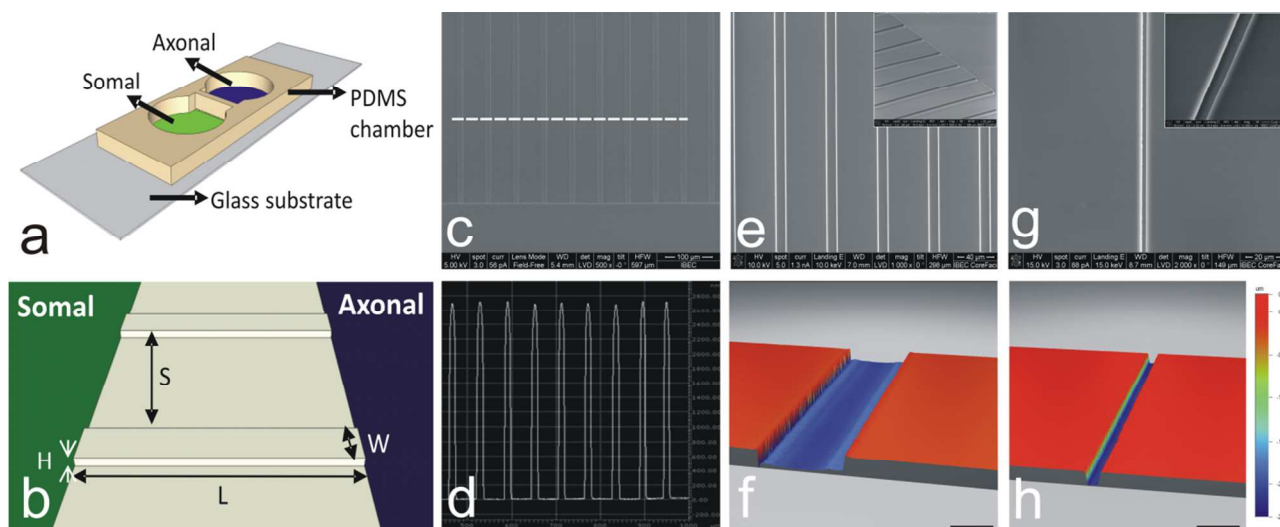


Fig. 1 Design and fabrication of microfluidic based open chamber co-culture system. a) Schematic drawing of co-culture system consisting of two open chambers ($\varnothing = 12$ mm) for culturing of motoneurons and C2C12-derived myotubes. The PDMS device was irreversibly bonded on top of glass slide by plasma bonding. b) The somal and axonal compartments are connected by a series of parallel microchannels ($W \times H \times L = 10 \mu\text{m} \times 2.7 \mu\text{m} \times 1$ mm) separated by a distance of $50 \mu\text{m}$. In the experiments of utilizing smaller channel dimensions, the width was modified to $2 \mu\text{m}$, while the other parameters were kept the same. SU8 photoresist features on glass slide masters were subjected to SEM (c) and profilometer (d) characterization. $10 \mu\text{m}$ (e, f) and $2 \mu\text{m}$ (g, h) wide PDMS channels were observed under SEM (e, g) and interferometer (f, h). Inserts of (e and g) were imaged under tilt condition using SEM. Scale bars in (f) and (h) are $5 \mu\text{m}$.

coverslip (Fig. 1a). The bonding was facilitated via the exposure of PDMS surface and glass slide with oxygen in a plasma chamber for surface activation creating an irreversible bonding. This strong bonding prevents leakage of the media into the other chamber, undesired alternative axonal pathways, and detachment of PDMS from the glass coverslip during long-term cell culture. The device contains a physical barrier with embedded microchannels ($L = 1$ mm) separating two large reservoirs ($\varnothing = 12$ mm), i.e., somal and axonal reservoirs (Fig. 1b). Media was changed every 2 to 3 days and no appreciable changes in cell viability or detectable liquid evaporation were observed. It took approximately one week in culture for motoneuron axons to cross the entire microchannels and to reach the adjacent reservoir. The width (W) and height (H) of the microchannels were measured to be $10 \mu\text{m}$ and $2.7 \mu\text{m}$ respectively, and separated (S) by $50 \mu\text{m}$ (Figs. 1b-f). This geometry allows neurites to enter microchannels but not the cell bodies due to physical constrains. The length of microchannels were chosen to be 1 mm because this length scale ensures that only axons were able to cross the entire microchannels and not dendrites.²⁴ In parallel, we have also designed and fabricated a device containing smaller microchannels ($W \times H = 2 \mu\text{m} \times 2.7 \mu\text{m}$) aiming for isolation of a low number of axons (Figs. 1g and h). However, with this dimension, it took approximately 2 weeks for the axons to cross the entire 1 mm long microchannels (ESI Fig. 1†).

Establishing a protocol for mixed co-culture of motoneuron–myotube

As an initial step to set up a co-culture protocol for in-chip system, we first analyzed culture conditions individually for motoneurons and myoblasts in current culture plates (see material and methods for details). After 8 days in culture, motoneurons exhibited typical stellate morphology in glass bottom petri dishes (Fig. 2a). Isolation of a pure population of

motoneurons is challenging, especially from embryonic mouse spinal cord. In fact, after optimizing the isolation protocol, we could still identify the presence of astrocytes (S100 β or GFAP-positive; Figs. 2b and 2c) and oligodendrocytes (olig2-positive, Fig. 2d) in our cultures. Nonetheless, we have noticed that motoneurons could actually improve their viability in the presence of those glial cells, which has also been previously reported.²⁸⁻³¹

C2C12 myoblast cell line is commonly used as a simplified model for studying muscular system since myoblast can be induced to form myotubes (Fig. 2e). A C2C12 myoblast to myotube differentiation protocol was optimized to characterize the differentiation process and to define the differentiation timing in a standard culture plates for later establishment of the co-culture in our chips. As observed in Figure 2f, matured and elongated differentiating myotubes from C2C12 cells express Myosin II. Once both cell cultures were optimized separately, we performed co-cultures testing in glass-bottomed petri dishes ($\varnothing = 12$ mm). Figure 2g shows bright-field micrograph of co-cultured condition showing two differentiated myotubes in proximity of several motoneurons. Motoneurons typically extend their axons over differentiated myotubes after 7 to 10 days culture *in vitro*. To demonstrate that axons and myotubes established synaptic connections, we performed Alexa Fluor 488–conjugated α -bungarotoxin (BTX) staining. BTX has high affinity to the α -subunit of the nicotinic acetylcholine receptor allowing for an accurate indication of NMJ formation. Microscopic observations of Alexa-BTX treated cultures showed the connections in mixed conditions by detecting the clusters of positive staining of BTX in identified myotubes (Figs. 2h and i).

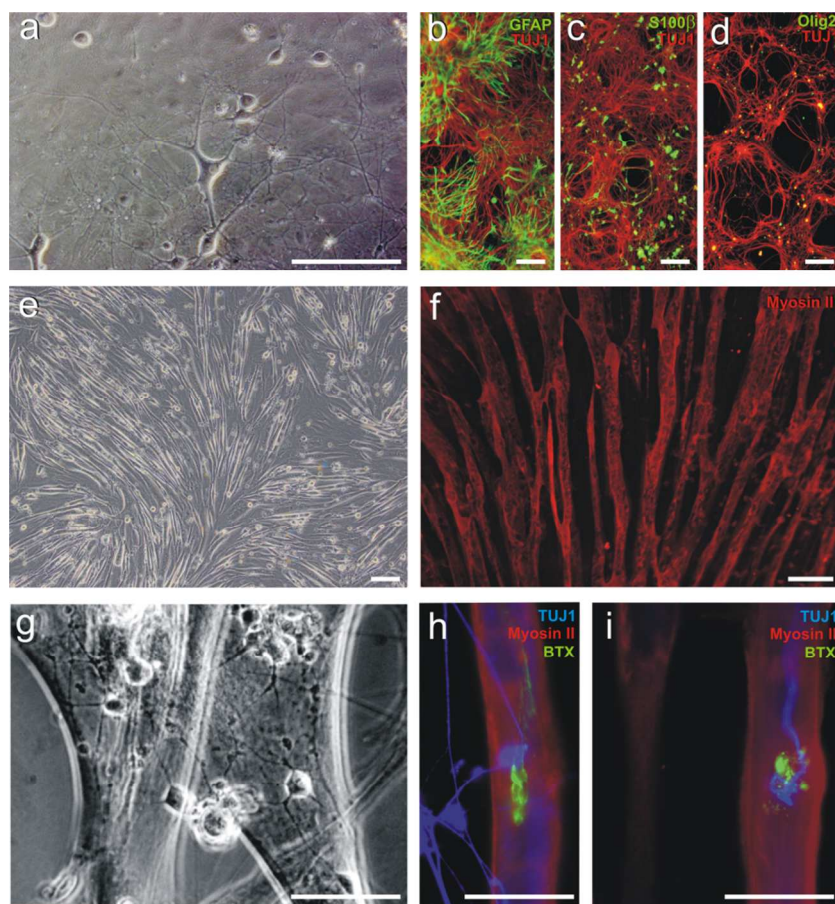


Fig. 2 Characterization of motoneuron and myotube co-culture on a single platform. a) Photomicrograph illustrating cultured embryonic mouse motoneurons growing over Poly-L-Ornithine and laminin coated coverslips (8 DIV). Notice the presence of glial cell monolayer under motoneurons. Mixed co-culture of motoneurons (α -TUJ1 positive) and glia stained with antibodies to (b) glial fibrillar acidic protein (GFAP), (c) S100 β and (d) oligodendrocyte transcription factor (olig2) at 8-10 DIV. Bright field micrographs of C2C12 myoblast cells differentiating into myotubes (e) and differentiated myotubes stained for Myosin II (f) in red. g) Phase contrast micrograph of mixed motoneurons and myotubes co-culture during 7-10 DIV. h-i) NMJ formations on glass bottom petri dishes (7-12 DIV) stained with Alexa-BTX, Myosin II and TUJ1. Scale bars: 100 μ m.

Viable co-culture and formation of NMJ in compartmentalized PDMS chips

Compartmentalized, fluidically-isolated microfluidic devices enable the cultures of motoneurons and C2C12 cells in two separated compartments connected by motoneuron axons. Highly reproducible co-cultures were established following the strict timeline protocol shown in Figure 3a. Motoneurons and differentiating C2C12-derived myotubes showed their typical morphologies and with high viabilities when cultured in our microfluidic devices (Fig. 3b). In addition, after 7 days *in vitro* culture, some of myotubes started to beat spontaneously in our chip (ESI Video 1†).

Motoneurons were seeded in somal compartment 1 day before seeding C2C12 myoblasts in counter compartment. 4 days later, Ara-C was added to complete motoneuron media (CMM), to decrease excessive glial proliferation. Despite the addition of essential growth factors to the CMM, the presence of those glial populations seems to be important for the maintenance of a healthy motoneuron culture. We have observed that when glial growth was blocked early (up to 24h) after plating motoneurons, the culture quality was largely compromised (data not shown). After approximately 6-7 DIV, axons from the somal compartment reached the axonal compartment. At the

same time, C2C12 cells began to differentiate. Finally, after 2 to 3 more days, the distal axons reached matured myotubes forming NMJs, comparable to what we observed previously in the mixed co-culture condition (Fig. 2). In order to improve both motoneuron survival and number of crossing axons, additional neurotrophins, BDNF and HGF, were added to CNTF and GDNF. The presence of the four neurotrophins has rendered a large number of axons crossing the microchannels (ESI Figs. 2a, b, and d†). Furthermore, we aimed to determine whether inhibitory molecules such as the class-3 secreted Semaphorin 3A (Sema3A) may also affect motoneuron axonal growth. It has been demonstrated that Sema3A impairs the growth of motoneuron axons.^{32,33} Experimentally, when Sema3A (1 μ g/ml) was added in the culture media we observed that axon growth was largely impeded and their entrance to the myotube compartment was significantly reduced compared to control experiments. (ESI Figs. 2c and d†).

Then, in order to determine whether transport processes, such as the organelle axonal transport occurs in chip culture, mitochondria were labelled with Mitotracker (ESI Fig. 3†). Results indicate the presence of Mitotracker-labelled mobile mitochondria along the axons inside the microchannels

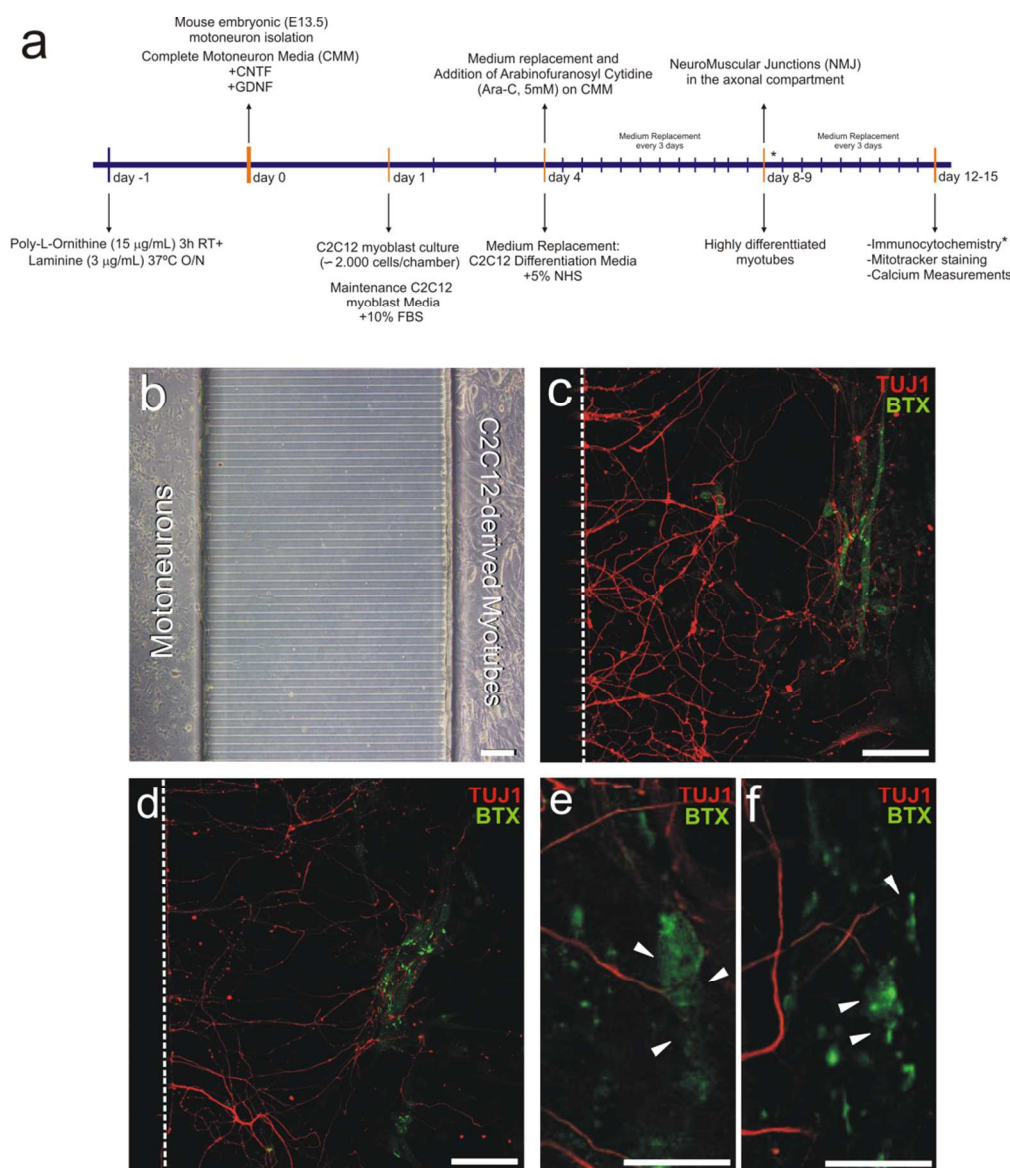


Fig. 3 NMJ formation in compartmentalized microfluidic devices. a) Timeline for establishing the co-culture of motoneurons and myotubes in chip. b) Phase contrast image of motoneurons (left) and C2C12 differentiating cells (right) in the separated compartments of a microfluidic device 5-6 DIV. c-d) Fluorescence micrographs of the co-culture in myotube compartment. After 12-15 DIV, the co-cultures showed a significant motoneuron axon outgrowth (TUJ1-positive) and connected with C2C12-derived myotubes establishing synapsis (Alexa-BTX staining). e-f) High magnification micrographs showing the motoneuron axons contacting with NMJs on myotubes visualized by Alexa-BTX (arrowheads). Scale bars: (b) 200 μm , (c) and (d) 100 μm , (e) and (f) 20 μm .

suggesting that normal axonal transport along the axon of motoneurons is maintained.

Next, to illustrate the synapse contacts resulted in the formations of functional NMJs in chip, we used Alexa-BTX staining (Figs. 3c and 3d) to identify AChR clusters on myotubes. High magnification micrographs in Figures 3e and 3f show two examples of confirmed neuromuscular synapse-like formations. We have identified several endings of axons interacting with myotubes forming a well-defined AChR clusters (indicated by arrow heads in Figures 3e and f).

Intracellular calcium (Ca^{2+}) transients in C2C12 myotubes after potassium chloride (KCl) incubation in cultured motoneurons in compartmentalized chips

We also aimed to test whether synapse transmission occurred in our chip. Thus, we performed an analysis of Ca^{2+} transients in differentiated myotubes via incubation with Fluo 4-AM when motoneurons were stimulated with 100 mM KCl.

First, as control experiments, we analyzed how Ca^{2+} transients were evoked directly by depolarization using 100 mM KCl in the C2C12-derived myotubes 8-10 DIV after differentiation. As illustrated in Figures 4a and 4b, KCl triggers a noticeable synchronous and fast intracellular Ca^{2+} increase in myotubes. In fact, this localized Ca^{2+} increase in the myotubes was transient

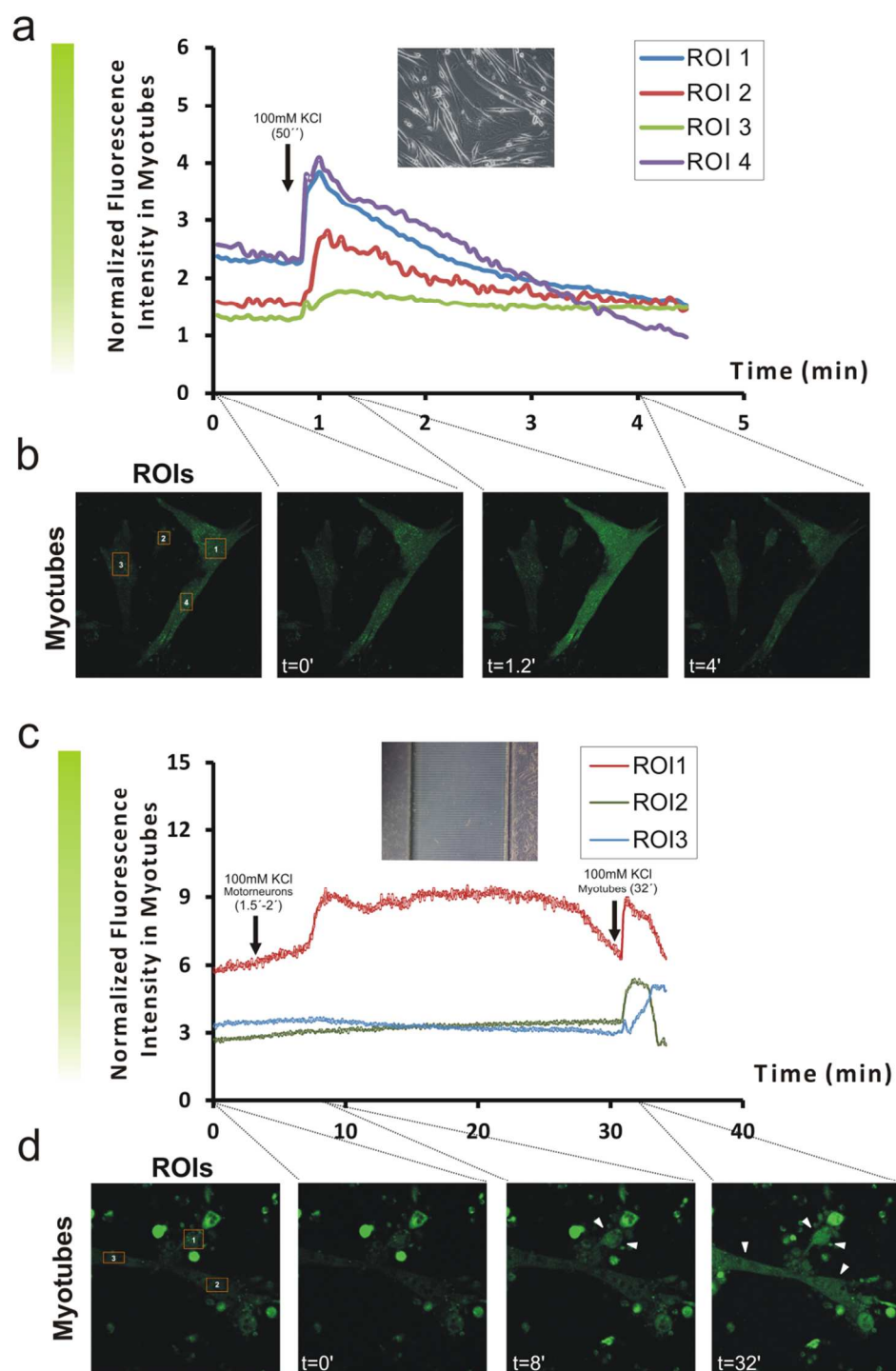


Fig. 4 Ca^{2+} transient generation in motoneuron-myotube co-cultures. **a**) Control experiment of C2C12 myotubes quickly synchronous responded to KCl (100 mM) stimulation ($t = 50'$, arrow) resulting Ca^{2+} transient peaks after the treatment (at $t = 1.2'$). **b**) Micrographs representing three time courses of the control experiment ($t = 0'$, $t = 1.2'$, $t = 4'$). At $t = 4$ minutes, the elevated fluorescence intensities have all reached basal level. Note, first micrograph shows the ROI distribution used for the analysis in (a). **c**) KCl (100 mM) stimulation on the motoneuron compartment induces Ca^{2+} transient in the C2C12-derived myotubes. Notice that we only observed an increase in the Ca^{2+} transient in the myotubes with functional connection with motoneuron axon (indicated by ROI1). After addition of the KCl ($t = 1.5 - 2'$, arrow), we observed a slow, gradual increase in the relative fluorescent intensity that reached a plateau after 8 minutes and sustained at the elevated level for 15 minutes. At $t = 30'$, the sustained Ca^{2+} transient returned to baseline. **d**) Micrographs representing three time courses of the actual experiment ($t = 0'$, $t = 8'$, $t = 32'$) as indicated in the x axis in (c). At $t = 32'$, myotube culture chamber was directly stimulated of with KCl (100 mM, arrow). Note, the first micrograph shows the ROI distributions used for the analysis in (c). Arrow heads indicate the myotubes that form functional connections with axons and maintained a sustained increase of Ca^{2+} . Fluorescent intensity levels were normalized by the background fluorescent noise.

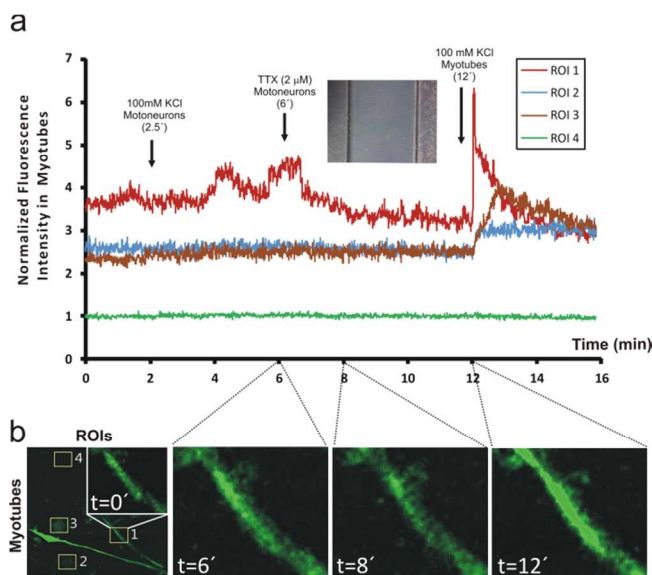


Fig. 5 TTX treatment reduces Ca^{2+} transient intensity in motoneuron-myotube co-culture in chip. a) Motoneuron compartment was stimulated with 100 mM KCl at $t = 2.5$ mins as shown in Figure 4 (arrow). TTX was added at $t = 6$ mins (arrow) to the KCl-treated motoneurons. Finally another dose of 100 mM KCl was added at $t = 12$ mins (arrow) in the C2C12 compartment. The graph shows the responses from the connected myotube (ROI 1), the unconnected myotubes ROI's 2 and 3, and the background ROI 4. The fluorescent intensity level was normalized to background noise. b) Zoom-in micrographs of connected myotubes (ROI 1) responses at $t = 0$, 6, 8, and 12 mins. Note, the first micrograph also shows the ROI distributions used for the analysis.

and showed a Ca^{2+} spike lasting a short duration and the fluorescence levels returned to baseline after 3 to 4 minutes as expected. We noticed that not all the myotubes responded equally to the KCl stimulation (i.e., exhibiting different levels of fluorescent intensity) but all responses were synchronous. Next, to confirm the absence of putative diffusion of KCl to the C2C12 reservoir, 100 mM KCl was added to the soma compartment (without motoneurons) and the Ca^{2+} transients in C2C12 plated in the second reservoir were analysed (ESI Video 2†). As expected, C2C12 myotubes growing in the axonal compartment showed a basal asynchronous activity that was not modified by the addition of KCl in the somal compartment demonstrating that compartmentalized chambers showed fluidic isolation. Due to the characteristics of high fluidic resistance in microchannels, a volume difference of the two compartments (higher fluid level in axonal compartment) induces a slow, but sustained, laminar net flow of fluid from axonal compartment to somal compartment through the microchannels without substantial modification of the composition in somal compartment. The net flow impairs the diffusion phenomena from somal to axonal compartment as also reported.²⁴

After we confirmed the positive response of C2C12 myotubes from direct stimulation by KCl and the fluidic isolation of the chambers, we induced the depolarization of the motoneurons cultured in the somal compartment with 100 mM KCl and recorded the fluorescent intensity change in myotube compartment (Figs. 4c and d). Figure 4c shows the Ca^{2+} level of a myotube (labelled ROI1) slowly increased with time and

sustained at an elevated level for 15 minutes before the intensity level fell down again. However, the other two myotubes (indicated by ROIs 2 and 3) in the same optical field were not observed to display any fluorescence intensity change. Finally, as a positive control, we added 100 mM KCl directly to the myotube compartment, and instantaneously, all the studied myotubes quickly responded synchronous to the direct KCl stimulation (Fig. 4c, at 32 minutes). Thus, we can conclude that fluorescence changes observed from myotube (labelled ROI1) was not an artefact. In fact, the ROI1 myotube was closer to the microchannel exits and it was very likely that ROI1 myotube form NMJs with an axon from somal compartment and the other two myotubes did not form connections. This prolonged, elevated fluorescent signal increase has also been observed in other repeated experiments (data not shown). Moreover, this KCl activation was specific since the addition of TTX (2 μM) after KCl stimulation strongly decreased the evoked Ca^{2+} -triggered fluorescence in C2C12 myotubes (Fig. 5).

Discussion

In this work, we have presented a modified compartmentalized microfluidics cell co-culture platform for generating robust and functional NMJ formations for further neurobiological studies. Using the present open chamber microfluidic setup has following advantages: 1) It provides improved nutrient and gas exchange to cell cultures with much more efficiency than cells growing under restricted environments such as inside a microchannel with a limited nutrient supply (e.g., see ESI Table 1†). 2) The open chamber enables simple manipulations to the cell culture, such as media exchange or introducing drugs, toxins or pharmacological reagents without the need of an external pump. 3) The cell culture area can be easily modified “on demand” by using different sizes of commercially available hole-punchers or cutters.

Our modified culture devices have two wells of 12 mm in diameter, which have the same dimension to those microplates commonly used in biological laboratories from several companies (Nunc, Costar, WPI, etc). This macro cell culture format can be quite important when culturing certain sensitive cell types, such as primary cortical neurons, neural stem cells or induced pluripotent stem cells allowing them to differentiate. At the same time, modification of the microstructure of the design (i.e., geometry of microchannels) can be easily attained to suit particular experimental applications. For instance, in our experiments the compartmentalization of the motoneurons is accomplished due to the small openings of microchannels.²⁴ Similarly, if we were interested to study the behaviour of low number of axons, we would be able to isolate those axons by reducing the dimension and the number of microchannels without additional changes in the culture conditions (ESI Fig. 1†). In some circumstances, a low number or single isolated axons can be valuable in interrogating some particular issues that yet to be solved due to the lack of specific tools. For example, it would be interesting to explore single axons electrical responses comparing to the group axons responses *in vitro*.³⁴⁻³⁶ Another interesting application of single axon isolation is the possibility to trace organelle or molecule transports in a low number of axons improving optical resolution and analysis. In addition, the resulting predetermined linear track and direction of transport enables a more accurate and easier way of quantification (ESI Fig. 3†).

In vitro methods to generate neuromuscular junction formation to study spinal or muscular diseases are typically mixed

cultures performed in a common plate with motoneurons and muscle cells receiving the same media. However, this type of co-culture system do not fully mimic the *in vivo* NMJ condition as those cell types are in different extracellular matrix environments and connected by peripheral nerves. Using an open chamber, compartmented, fluidically controlled isolation microdevice, we have successfully cultured those two cell types in separated compartments and receiving individual distinct culture media and joined solely by axonal processes. We have established a robust culture protocol to generate healthy, long-term survival of the cell co-cultures in chip (up to 4 weeks). Furthermore, NMJ formation in differentiated myotubes was verified by the positive staining of Ach receptors via imaging through Alexa-BTX staining.

In addition, myotubes were able to form spontaneous contractions in our culture chips (ESI Video 1†). This was further modulated by the generation of Ca^{2+} transient in cultured myotubes after KCl stimulation of motoneurons. KCl treatment triggers motoneurons to release neurotransmitters which induces Ca^{2+} transient in the connected myotubes. From our control experiments, where myotubes were directly stimulated with KCl, we observed the duration of Ca^{2+} changes lasted less than 1 minute. This instantaneous and transient Ca^{2+} changes for myotubes stimulation was commonly observed. However, when KCl stimulation applied to motoneurons, we have observed the prolonged Ca^{2+} response (more than 15 minutes) in the myotube compartment. To rule out the possibility of sustained Ca^{2+} influx was triggered by the diffused KCl from motoneuron compartment, we have conducted a detailed diffusion experiments (Fig. 5). In addition, not all analyzed myotubes respond in the same way, indicating a specific effect of the KCl stimulation in particular motoneurons. Furthermore, the application of TTX on the motoneuron compartment resulted in diminishment of the fluorescent signal in myotube which was initially evoked by KCl stimulation on motoneurons (Fig. 5). Hence, the sustained elevated Ca^{2+} signals of the myotubes were caused by the specific stimulation from motoneurons. In fact, a protracted Ca^{2+} transient phenomenon has also been reported in striatal neurons and other cells when they were exposed directly to nitric oxide.³⁷

Conclusions

In conclusion, we have presented here an open microfluidic cell culture platform for the application of co-culture of motoneuron and C2C12-derived muscle cells aiming for generating a robust *in vitro* model of NMJ formations. Furthermore, we have shown to be able to manipulate a single cell population, i.e., motoneurons, and have proven the functional response via Ca^{2+} live imaging. Our modified macro-well microfluidic device will be especially useful for culturing environmental sensitive cells such as neurons and neural stem cells. Furthermore, with a simple modification of the design, we can set up a more sophisticated co-culture platform to study more complex neuron interactions.

Acknowledgements

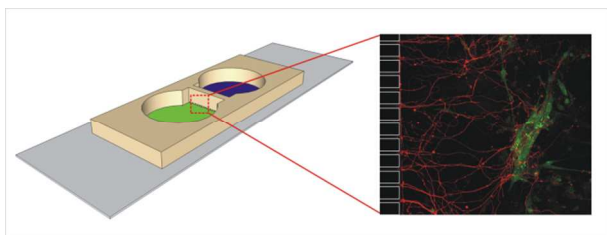
The authors thank Asumpció Bosch (Department of Biochemistry and Molecular Biology, Autonomous University of Barcelona) for technical support on motoneuron culture. The authors also thank David Izquierdo and Juan Manuel Alvarez from IBEC Nanobioengineering group and Miriam Segura

From Molecular and Cellular Neurobiotechnology group to their technical assistances and Tom Yohannan for linguistic advice. The authors would also thank IBEC Core Facility staff for their generous help. This research was supported by the Botin Foundation, Seventh Framework Programme of the European Commission, grant agreement 222887, FP7-PRIORITY, the Spanish Ministry of Science and Innovation (BFU2012-32617), the Fundación Vasca de Innovación e Investigación Sanitarias (BIO12/AL/004) and the Generalitat de Catalunya (SGR2012-1218), La Caixa Obra Social Foundation (LCOSF), and the Instituto de Salud Carlos III (PI11/03028). CIBER-BBN is an initiative funded by the VI National RDi Plan 2008-2011, Iniciativa Ingenio 2010, Consolider Program, CIBER Actions and financed by the Instituto de Salud Carlos III with assistance from the European Regional Development Fund. JADR and OS were supported by MINECO, IBEC (Strategic Research Initiative program founded by LCOSF) and CIBERNED. The Nanobioengineering group has also supported from the Commission for Universities and Research of the Department of Innovation, Universities, and Enterprise of the Generalitat de Catalunya (SGR2012-1442).

References

1. P. L. Cheng and M. M. Poo, *Annu Rev Neurosci*, 2012, 35, 181-201.
2. A. P. Barnes and F. Polleux, *Annu Rev Neurosci*, 2009, 32, 347-381.
3. A. C. Horton and M. D. Ehlers, *Neuron*, 2003, 40, 277-295.
4. L. de la Torre-Ubieta and A. Bonni, *Neuron*, 2011, 72, 22-40.
5. C. G. Dotti and M. M. Poo, *Nat Cell Biol*, 2003, 5, 591-594.
6. B. DuBoff, M. Feany and J. Gotz, *Trends Neurosci*, 2013, 36, 325-335.
7. P. H. Reddy, *Brain Res*, 2011, 1415, 136-148.
8. A. H. Schapira, V. M. Mann, J. M. Cooper, D. Krige, P. J. Jenner and C. D. Marsden, *Ann Neurol*, 1992, 32 Suppl, S116-124.
9. S. Boillee, C. Vande Velde and D. W. Cleveland, *Neuron*, 2006, 52, 39-59.
10. F. Palau, A. Estela, D. Pla-Martin and M. Sanchez-Piris, *Adv Exp Med Biol*, 2009, 652, 129-137.
11. D. Y. Lu, C. H. Tang, W. L. Yeh, K. L. Wong, C. P. Lin, Y. H. Chen, C. H. Lai, Y. F. Chen, Y. M. Leung and W. M. Fu, *Eur J Pharmacol*, 2009, 613, 146-154.
12. A. M. Taylor, N. C. Berchtold, V. M. Perreau, C. H. Tu, N. Li Jeon and C. W. Cotman, *J Neurosci*, 2009, 29, 4697-4707.
13. J. M. Peyrin, B. Deleglise, L. Saias, M. Vignes, P. Gougis, S. Magnifico, S. Betuing, M. Pietri, J. Caboche, P. Vanhoutte, J. L. Viovy and B. Brugg, *Lab on a chip*, 2011, 11, 3663-3673.
14. U. Hengst, A. Deglincerti, H. J. Kim, N. L. Jeon and S. R. Jaffrey, *Nat Cell Biol*, 2009, 11, 1024-1030.
15. J. Park, H. Koito, J. Li and A. Han, *Lab on a chip*, 2012, 12, 3296-3304.
16. E. Park, J. D. Bell and A. J. Baker, *CMAJ*, 2008, 178, 1163-1170.
17. P. Shi, M. A. Scott, B. Ghosh, D. Wan, Z. Wissner-Gross, R. Mazitschek, S. J. Haggarty and M. F. Yanik, *Nature communications*, 2011, 2, 510.
18. T. T. Kanagasabapathi, P. Massobrio, R. A. Barone, M. Tedesco, S. Martinoia, W. J. Wadman and M. M. Decre, *J Neural Eng*, 2012, 9, 036010.

19. T. T. Kanagasabapathi, K. Wang, M. Mellace, G. J. Ramakers and M. M. Decre, *Conference proceedings : ... Annual International Conference of the IEEE Engineering in Medicine and Biology Society. IEEE Engineering in Medicine and Biology Society. Conference*, 2009, 2009, 1655-1658.
20. M. Das, J. W. Rumsey, C. A. Gregory, N. Bhargava, J. F. Kang, P. Molnar, L. Riedel, X. Guo and J. J. Hickman, *Neuroscience*, 2007, 146, 481-488.
21. M. Das, J. W. Rumsey, N. Bhargava, M. Stancescu and J. J. Hickman, *Biomaterials*, 2010, 31, 4880-4888.
22. H. S. Park, S. Liu, J. McDonald, N. Thakor and I. H. Yang, *Conference proceedings : ... Annual International Conference of the IEEE Engineering in Medicine and Biology Society. IEEE Engineering in Medicine and Biology Society. Conference*, 2013, 2013, 2833-2835.
23. K. A. Southam, A. E. King, C. A. Blizzard, G. H. McCormack and T. C. Dickson, *J Neurosci Methods*, 2013, 218, 164-169.
24. A. M. Taylor, M. Blurton-Jones, S. W. Rhee, D. H. Cribbs, C. W. Cotman and N. L. Jeon, *Nat Methods*, 2005, 2, 599-605.
25. R. B. Campenot, *Methods Enzymol*, 1979, 58, 302-307.
26. M. Arundell, V. H. Perry and T. A. Newman, *Lab on a chip*, 2011, 11, 3001-3005.
27. J. Park, J. Li and A. Han, *Biomedical microdevices*, 2010, 12, 345-351.
28. M. C. Bohn, *Experimental neurology*, 2004, 190, 263-275.
29. M. Sendtner, Y. Arakawa, K. A. Stockli, G. W. Kreutzberg and H. Thoenen, *Journal of cell science. Supplement*, 1991, 15, 103-109.
30. G. M. Gilad, V. H. Gilad, D. Dahl and A. Bignami, *Brain research*, 1988, 458, 249-260.
31. A. R. Taylor, M. B. Robinson and C. E. Milligan, *Nature protocols*, 2007, 2, 1499-1507.
32. R. J. Pasterkamp, F. De Winter, R. J. Giger and J. Verhaagen, *Progress in brain research*, 1998, 117, 151-170.
33. R. J. Pasterkamp, R. J. Giger and J. Verhaagen, *Experimental neurology*, 1998, 153, 313-327.
34. E. Claverol-Tinture, J. Cabestany and X. Rosell, *IEEE transactions on bio-medical engineering*, 2007, 54, 331-335.
35. R. Morales, M. Riss, L. Wang, R. Gavin, J. A. Del Rio, R. Alcubilla and E. Claverol-Tinture, *Lab on a chip*, 2008, 8, 1896-1905.
36. L. Wang, M. Riss, J. O. Buitrago and E. Claverol-Tinture, *Journal of neural engineering*, 2012, 9, 026010.
37. T. F. Horn, G. Wolf, S. Duffy, S. Weiss, G. Keilhoff and B. A. MacVicar, *FASEB J*, 2002, 16, 1611-1622.
38. G. M. Whitesides, E. Ostuni, S. Takayama, X. Jiang and D. E. Ingber, *Annual review of biomedical engineering*, 2001, 3, 335-373.



A large open-reservoir, fluidically-isolated, compartmentalized microfluidic co-culture platform was utilized as an *in vitro* model for establishing neuro-muscular junction formation.